Steel and Composite Structures, *Vol. 32, No. 2 (2019) 173-187*
DOI: https://doi.org/10.12989/scs.2019.32.2.173

On buckling analysis of laminated composite plates using a nonlocal refined four-variable model

Davood Shahsavari, Behrouz Karami* and Maziar Janghorban

Department of Mechanical Engineering, Marvdasht Branch, Islamic Azad University, Marvdasht, Iran

(*Received December 11, 2018, Revised March 13, 2019, Accepted June 12, 2019*)

Abstract. This study is concerned with the stability of laminated composite plates modelled using Eringen's nonlocal differential model (ENDM) and a novel refined-hyperbolic-shear-deformable plate theory. The plate is assumed to be lying on the Pasternak elastic foundation and is under the influence of an in-plane magnetic field. The governing equations and boundary conditions are obtained through Hamilton's principle. An analytical approach considering Navier series is used to fine the critical bucking load. After verifying with existing results for the reduced cases, the present model is then used to study buckling of the laminated composite plate. Numerical results demonstrate clearly for the first time the roles of size effects, magnetic field, foundation parameters, moduli ratio, geometry, lay-up numbers and sequences, fiber orientations, and boundary conditions. These results could be useful for designing better composites and can further serve as benchmarks for future studies on the laminated composite plates.

Keywords: composite structures; buckling; magnetic field; Eringen nonlocal differential model

1. Introduction

Due to the need of an improved and more efficient structure for use in industrials likewise aerospace, nuclear, automobile and civil, the trend of using laminated composite structures significantly grown during the last few years because of their superior properties such like flexibility in design, low cost, high corrosion resistance, high fatigue life, tailor-made properties, bend extensional and high strength to weight proportion (Gibson 2016). However, in comparison to isotropic material structures, laminated composite ones by combining together two (or more) constituents which it leads to enhancement in number of involved variables and the intrinsic anisotropy behavior of the individual layers usually are more complex structures (Reddy 2004). Hence, optimal design of these structures needs an efficient mathematical model in practice.

As far as the structural mechanics is concerned, laminated composites are broadly used as main constituents of beams shells and plates because of their fantastic properties like bend extensional and high strength to weight proportion. In recent years, extensive studies relevant to performance of laminated composite structures have been conducted using the classical continuum theories (Sayyad and Ghugal 2015). Among these theories, classical plate theory (CPT) despite possessing the simple constitutive equations and providing the accurate solution in most cases, cannot consider the possible influence of rotary inertia and transverse shear deformations included in the thick plates. Moreover, laminated composites due to their low transverse shear modulus are having inadequate strength in shear, which it should be reckon. To overcome these limitations, the first-order-shear-deformation theory (FSDT) was introduced for both thin and thick plates; however, its accuracy depends strongly on the shear correction factor. Furthermore, the stress variation in the laminated composite plate based on the FSDT was not acceptable (Rank *et al*. 1998). Thus, various higher-order-shear-deformation theories (HSDTs) have been suggested which include different shape functions along with a variable number of unknown equations. These theories were successfully applied to investigate more accurately the response of different advanced composite plates such as laminated-sandwich-functionally graded plates. However, these theories are associated with many more equilibrium equations, increasing substantially the complexity of the problem analysis. Accordingly, simple theories including fewer unknowns are much appealing. In order to minimize the total number of variables used in the equilibrium equations, (Shimpi 2002) proposed a refined model with only two variables for the study of isotropic plates (or refined-plate theory (RPT)). Afterward this model has been developed for orthotropic (Shimpi and Patel 2006), FGM (Mechab *et al*. 2010, Zidi *et al*. 2014), and laminated composite plates (Thai and Kim 2012). Next, various models of RPT with different shape functions through dividing the transverse displacement into bending and shear parts were suggested for mechanical response (i.e., static, dynamic and stability) of micro/nano-plate-like structures (Houari *et al*. 2016, Sadoun *et al*. 2018, Boukhari *et al*. 2016, Fourn *et al*. 2018, Beldjelili *et al*. 2016, Hirwani *et al*. 2018, Hachemi *et al*. 2017, Katariya and Panda 2016, Shahsavari and Janghorban 2017).

*Corresponding author, Ph.D. Student,
E-mail: behrouz.karami@miau.ac.ir

ISSN: 1229-9367 (Print), 1598-6233 (Online)

Buckling phenomena are both necessary and destructive. This phenomenon is a mechanical characteristic which may occur when the structure is subjected to loads in its plane. Although uniaxial or biaxial compressive loads are most frequently considered, buckling sometimes occurs with biaxial loads in which a compressive load is defined in one direction and tensile load in the other one, or subjected to shearing loads or a combination of these forms of loading. On the other hand, buckling or stability of engineering structures like beam/plate/shells may occur in a different forms including global or local deflections, while it might lead to the collapse of the structures. Consequently, predicting the measure of buckling failure is an essential task in design of structural components. Having said that, the pioneered studies were mainly focused on uniaxial and biaxial buckling; however, a great deal of attention has been devoted to study shear buckling, thermal buckling and post-buckling examination of these structures in terms of both linear and non- linear (Bousahla *et al*. 2016, Kolahdouzan *et al*. 2018, Mehar *et al*. 2019, Kar *et al*. 2016, 2017, Kar and Panda 2017, Panda and Singh 2013b, Katariya *et al*. 2017, 2018, Panda and Singh 2013a, Kar and Panda 2016, Karami and Karami 2019, Karami and Shahsavari 2019, Shahsavari *et al*. 2018a, Karami *et al*. 2018d). But surprisingly, there is a limitation on size-dependent buckling analysis of laminated composite structures including elastic foundation.

Application of beams/plates rests on elastic foundation has been found in micro-electromechanical systems (MEMS) (Maluf and Williams 2004). Up to now, various hypotheses of elastic foundation models for expressing the interaction amongst foundation and plate have been introduced. The popular elastic foundation models includes Winkler elastic foundation (Winkler 1867) with only one coefficient substrate reaction (spring layer) and Pasternak model (Pasternak 1954) containing two-parameter substrate (spring and shear layers). Hence, a wide range of studies regrading micro/nanostructures due to distributed reaction between both above-elastic foundation models and the lower surface of soft plates with various distributions of material properties has been conducted (Shahsavari *et al*. 2018d, Asemi and Shariyat 2016).

Although the classical continuum theories have used for modeling the mechanical behavior of different structures such as beams, plates and shells with macroscale (Pacoste and Eriksson 1997, Babuška and Li 1992), many other problems in small scales cannot be suitably solved by the classical approach (Stamoulis and Giannakopoulos 2012). This is because, in the classical continuum theories, the length-scale parameters (known as size effects) are missing, which demonstrate the microstructure and atomic structure of the body (Askes and Aifantis 2011). To include these length-scale parameters, several continuum theories, known as generalized continuum theories or size-dependent continuum theories were developed, which contain different numbers of length-scale parameters. One of the oldest theories with several length-scale parameters was derived by (Cosserat 1909). Following their work, different types of theories were proposed. Some of these theories considered the size effects such as nonlocal and strain gradient theories, and modified couple stress and strain theories. Recently developed theories seem to be more suitable for engineering applications because of their simplicity compared to the old ones. Hence, there are many works which have been carried out on these models (Farajpour *et al*. 2018, 2019, Farokhi and Ghayesh 2018a, b, 2015a, b, 2016, Ghayesh 2018, She *et al*. 2019, Karami *et al*. 2019f, Shahsavari *et al*. 2018b, c, Karami *et al*. 2018b, c, 2019a, b, c, d, e, Karami and Janghorban 2019, Ghayesh *et al*. 2016, 2017a, b, 2018, Gholipour *et al*. 2015, She *et al*. 2018). One of these theories with only one length-scale parameter is the nonlocal elasticity theory (NET) (Eringen and Edelen 1972) which has been adopted by several researchers for studying various structures such as single-walled and double-walled nanotubes (Zhang *et al*. 2005) nanoshells (Ghavanloo and Fazelzadeh 2013, Arefi 2018), nanobeams (Aydogdu 2009, Lim 2010), and nanoplates (Pradhan and Phadikar 2009, Mehar *et al*. 2018, Karami *et al*. 2018a). More recently, (Shahsavari *et al*. 2017) examined the free and forced vibration response of nanoplates rested on visco-elastic foundation under moving load on the basis of NET using state-space method. Furthermore, An analytical solution was developed by (Raghu *et al*. 2016) for laminated composite plates using a third-order shear deformation theory on the basis of nonlocal elasticity theory which considers both the nonlocal and surface stress effects, with applications to vibration and bending analyses.

In this article, we consider cross-ply, angle-ply, and symmetric and antisymmetric laminated composite plates embedded within elastic Pasternak foundation. The presented research will be focused on the size-dependent critical uniaxial/biaxial buckling under the influence of in-plane magnetic field. The axial, bending and shear effects are taken into account using a novel refined plate theory in conjunction with the ENDM, which will be clearly addressed. The equations of motion are derived in Section 3 based on Hamilton's principle. In Section 4, analytical solutions are presented for both cross-ply and angle-ply laminated composite plates. In Section 5, a comprehensive parametric study will be carried out to demonstrate the impact of laminated plate geometry (length, width, and thickness), foundation parameters (spring and shear layer), size-dependence effect (nonlocal parameter), external loads (in-plane magnetic field), lay-up numbers (number of constitutive layers), fiber orientations (angles in constitutive layers), lay-up sequences of layers (symmetric and antisymmetric arrangements) and boundary condition (SS-1 and SS-2), on the buckling response. Finally, crucial conclusions are listed in Section 6. The novelties of this article may be summarized as follows:

(1) Size-dependent uniaxial and biaxial response of laminated composite plates are investigated for the first time.
(2) Up to now, the role of in-plane magnetic field has not been studied for any mechanical response of laminated composite structures.
(3) Coupling effects between bending and shear deformation are included for the modeling of nanostructure systems based on a novel refined-

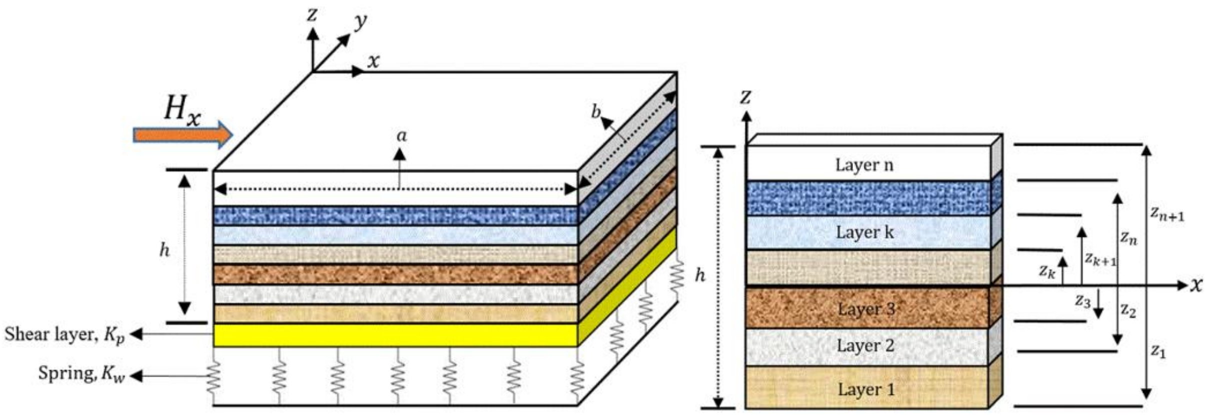

Fig. 1 A laminated composite plate subjected to an in-plane magnetic field

hyperbolic-shear-deformable plate theory.

(4) The size-dependent buckling analysis of cross-ply and angle-ply laminated composite plates are examined to show the impact of various lay-up numbers (number of constitutive layers), lay-up sequences of layers (symmetric and antisymmetric arrangements), fiber orientations (angles in constitutive layers), as well as boundary conditions.

(5) Even though the presented solution is based on Navier solution method, it completely supports the results of pioneer studies based on numerical methods (Finite Element Method FEM and Differential Quadrature Method DQM) and analytical methods.

2. Preliminary concepts and definitions

2.1 Problem definition

Stability of advanced structures under an external field is of vital importance in designing these structures where their buckling should be suitably controlled. Hence, we consider a multilayered composite plate resting on a Pasternak foundation displayed in Fig. 1 where the laminated composite plate is referred to a (x, y, z) set of coordinates with z-axis along the thickness direction.

To consider the magnetic force, an in-plane magnetic field induced by the Lorentz force is applied in x-direction, along with the in-plane mechanical forces as shown in Fig. 2.

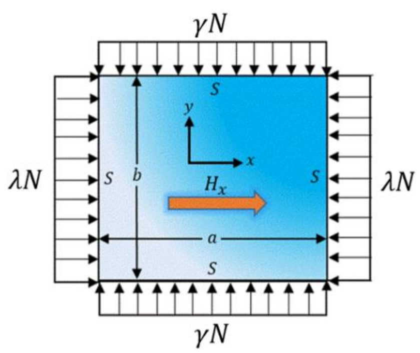

Fig. 2 A rectangular plate subjected to in-plane loads

2.2 Nonlocal elasticity theory

The nonlocal elasticity theory (Eringen and Edelen 1972), unlike the local theory, assumes that the stress at a point depends not only on the strain there but also on strains at all other points of the body. Therefore, nonlocal stress tensor is defined by

$$\tau_{ij} = \int_V \alpha\left(\left|\mathbf{x}'-\mathbf{x}\right|\right),\tau)\sigma_{ij}(x')d(V') \tag{1}$$

where $\sigma_{ij}(x)$, $\varepsilon_{kl}(x)$ are the local stress and strain tensors, $\alpha(|x' - x|)$ denotes the kernel function that is normalized over the volume of the body. Also in Eq. (1), τ is a material constant defined as (e_0/l) in which e_0 is a constant for adjusting the model in confirming some valid results by MD simulation or experiments model, a and l are intrinsic characteristics length and external characteristics length, respectively (Gopalakrishnan and Narendar 2013). For bounded continuous structures the law of strain-driven nonlocal integral (Eq. (1)) is not applicable and does not have analytical solutions in most technical interesting cases (Peddieson *et al*. 2003). Thus, in this paper, in order to model the size effects, the following differential fundamental relation is applied

$$(1-\mu\nabla^2)\sigma_{ij} = C_{ijkl}\,\varepsilon_{kl} \tag{2}$$

in which the two-dimensional Laplacian operator is defined as $\nabla^2 = \dfrac{\partial^2}{\partial x^2} + \dfrac{\partial^2}{\partial y^2}$, and μ is the nonlocal parameter. We further notice that the nonlocal parameter is affected by the boundary conditions, mode shapes, and type of motion, among others (Gopalakrishnan and Narendar 2013).

2.3 Refined-hyperbolic-shear-deformable-plate theory

In the formulation of the present refined-hyperbolic-shear-deformation-plate theory, the displacement fields are obtained based on the following assumptions (Zidi *et al*. 2014, Benachour *et al*. 2011, Bourada *et al*. 2012):

(1) The total transverse displacement is divided into bending and shear components, with both of them being functions of coordinates *x*, *y* and time *t* only.
(2) The in-plane displacements are divided into bending and shear parts. It is shown that the in-plane displacements are functions of *x*, *y*, *t* and *z* in which the bending part is the same as that in the CPT, but the shear part is in hyperbolic variation in thickness direction.

Then, the displacement fields can be assumed as

$$\begin{aligned} u(x,y,z,t) &= u_0(x,y,t) - z\frac{\partial w_b}{\partial x} - \psi(z)\frac{\partial w_s}{\partial x} \\ v(x,y,z,t) &= v_0(x,y,t) - z\frac{\partial w_b}{\partial y} - \psi(z)\frac{\partial w_s}{\partial y} \\ w(x,y,t) &= w_b(x,y,t) + w_s(x,y,t) \end{aligned} \quad (3)$$

where u_0 and v_0 are the displacements of the middle plane of the plate, and $\psi(z)$ defines the shape function determining the transverse shear strain changes along the thickness direction, assumed as (Shahsavari *et al*. 2018d)

$$\psi(z) = -\left(\begin{array}{l} \left(\dfrac{\cosh(1/2)}{24\sinh(1/2) - 11\cosh(1/2)} - 1\right)\left(\dfrac{z}{h}\right) \\ -\left(\dfrac{1}{24\sinh(1/2) - 11\cosh(1/2)}\right)\sinh\left(\dfrac{z}{h}\right) \end{array} \right) h \quad (4)$$

3. Theoretical formulations

From Eq. (3) the strain-displacement relations can be obtained as follows

$$\begin{aligned} \begin{Bmatrix} \varepsilon_{xx} \\ \varepsilon_{yy} \\ \gamma_{xy} \end{Bmatrix} &= \begin{Bmatrix} \varepsilon_{xx}^0 \\ \varepsilon_{yy}^0 \\ \gamma_{xy}^0 \end{Bmatrix} + z \begin{Bmatrix} \kappa_{xx}^b \\ \kappa_{yy}^b \\ \kappa_{xy}^b \end{Bmatrix} + \psi(z) \begin{Bmatrix} \kappa_{xx}^s \\ \kappa_{yy}^s \\ \kappa_{xy}^s \end{Bmatrix} \\ \begin{Bmatrix} \gamma_{yz} \\ \gamma_{xz} \end{Bmatrix} &= g(z) \begin{Bmatrix} \gamma_{yz}^s \\ \gamma_{yz}^s \end{Bmatrix} \end{aligned} \quad (5)$$

where

$$\begin{aligned} &\begin{Bmatrix} \varepsilon_{xx}^0 \\ \varepsilon_{yy}^0 \\ \gamma_{xy}^0 \end{Bmatrix} = \begin{Bmatrix} \dfrac{\partial u_0}{\partial x} \\ \dfrac{\partial v_0}{\partial y} \\ \dfrac{\partial u_0}{\partial y} + \dfrac{\partial v_0}{\partial x} \end{Bmatrix}, \begin{Bmatrix} \kappa_{xx}^b \\ \kappa_{yy}^b \\ \kappa_{xy}^b \end{Bmatrix} = \begin{Bmatrix} -\dfrac{\partial^2 w_b}{\partial^2 x} \\ -\dfrac{\partial^2 w_b}{\partial^2 y} \\ -2\dfrac{\partial^2 w_b}{\partial x \partial y} \end{Bmatrix} \\ &\begin{Bmatrix} \kappa_{xx}^s \\ \kappa_{yy}^s \\ \kappa_{xy}^s \end{Bmatrix} = \begin{Bmatrix} -\dfrac{\partial^2 w_s}{\partial^2 x} \\ -\dfrac{\partial^2 w_s}{\partial^2 y} \\ -2\dfrac{\partial^2 w_s}{\partial x \partial y} \end{Bmatrix} \begin{Bmatrix} \gamma_{yz}^s \\ \gamma_{xz}^s \end{Bmatrix} = \begin{Bmatrix} \dfrac{\partial w_s}{\partial y} \\ \dfrac{\partial w_s}{\partial x} \end{Bmatrix} \\ &g(z) = 1 - \frac{d\psi(z)}{dz} \end{aligned} \quad (6)$$

3.1 Constitutive equations

In this paper, the laminated plate is made of composite materials that constituent layer of elastic orthotropic properties. It can be made of several unidirectional plies accumulated in different orientations. Orthotropic axes in each lamina (indicated by superscript *k*) are oriented at an arbitrary angle θ to the (global) plate axis. Using the nonlocal elasticity relation (Eq. (2)), the constitutive relations (between nonlocal stresses and strains) for each layer in the global coordinates can be expressed as (Raghu *et al*., 2016).

$$\begin{bmatrix} (1-\mu\nabla^2)\sigma_{xx} \\ (1-\mu\nabla^2)\sigma_{yy} \\ (1-\mu\nabla^2)\tau_{xy} \\ (1-\mu\nabla^2)\tau_{yz} \\ (1-\mu\nabla^2)\tau_{xz} \end{bmatrix} = \begin{bmatrix} \bar{Q}_{11} & \bar{Q}_{12} & \bar{Q}_{16} & 0 & 0 \\ \bar{Q}_{12} & \bar{Q}_{22} & \bar{Q}_{26} & 0 & 0 \\ \bar{Q}_{16} & \bar{Q}_{26} & \bar{Q}_{66} & 0 & 0 \\ 0 & 0 & 0 & \bar{Q}_{44} & \bar{Q}_{45} \\ 0 & 0 & 0 & \bar{Q}_{45} & \bar{Q}_{55} \end{bmatrix} \begin{Bmatrix} \varepsilon_{xx} \\ \varepsilon_{yy} \\ \gamma_{xy} \\ \gamma_{yz} \\ \gamma_{xz} \end{Bmatrix} \quad (7)$$

Now, under the rotation of an angle θ around *z*-axis in the *x*-*y* plane (measured counterclockwise from the fiber direction with respect to the positive *x*-axis), the transformation formulas for the stiffness are as (Reddy, 2004)

$$\begin{aligned} &\begin{bmatrix} \bar{Q}_{11} \\ \bar{Q}_{12} \\ \bar{Q}_{22} \\ \bar{Q}_{16} \\ \bar{Q}_{26} \\ \bar{Q}_{66} \end{bmatrix} = \begin{bmatrix} c^4 & 2c^2s^2 & s^4 & 0 & 4c^2s^2 \\ c^2s^2 & c^4+s^4 & c^2s^2 & 0 & -4c^2s^2 \\ s^4 & 2c^2s^2 & c^4 & 2c^2s^2 & 0 \\ c^3s & cs\left(-c^2-s^2\right) & -cs^3 & 0 & 2cs\left(-c^2+s^2\right) \\ cs^3 & cs\left(c^2-s^2\right) & -c^3s & 0 & 2cs\left(c^2-s^2\right) \\ c^2s^2 & -2c^2s^2 & c^2s^2 & 0 & c^2s^2\left(c^2s^2-2\right) \end{bmatrix} \begin{bmatrix} C_{11} \\ C_{12} \\ C_{22} \\ C_{16} \\ C_{66} \end{bmatrix} \\ &\begin{bmatrix} \bar{Q}_{44} \\ \bar{Q}_{45} \\ \bar{Q}_{55} \end{bmatrix} = \begin{bmatrix} c^2 & s^2 \\ -cs & cs \\ s^2 & c^2 \end{bmatrix} \begin{bmatrix} C_{44} \\ C_{55} \end{bmatrix} \end{aligned} \quad (8)$$

in which $c = \cos(\theta)$, $s = \sin(\theta)$; C_{ij} (in terms of the Voigt notation for the stiffness) are the reduced stiffness coefficients which can be further expressed in terms of the engineering constants in the material layer as

$$\begin{aligned} C_{11} &= \frac{E_1}{1-\nu_{12}\nu_{21}}, C_{12} = \frac{\nu_{12}E_2}{1-\nu_{12}\nu_{21}} \\ C_{22} &= \frac{E_2}{1-\nu_{12}\nu_{21}}, C_{66} = G_{12} \\ C_{44} &= G_{23}, C_{55} = G_{13}, \nu_{21} = \frac{E_2}{E_1}\nu_{12} \end{aligned} \quad (9)$$

3.2 Governing equations

The Hamilton's energy principle is applied to derive the equation of motion of the plate

$$\int_0^t \delta\left(-U_P - U_F + V\right)dt = 0 \tag{10}$$

in which δ indicates a variation, and U_P, U_F, and V are the strain energy of the plate, the energy due to the elastic foundation, and work done by the external force, respectively. These terms are derived below one by one.

3.2.1 Strain energy

First, the variation of the strain energy of the plate can be expressed as

$$\delta U_P = \int_V \begin{pmatrix} \sigma_{xx}\delta\varepsilon_{xx} + \sigma_{yy}\delta\varepsilon_{yy} + \tau_{xy}\delta\gamma_{xy} \\ +\tau_{xz}\delta\gamma_{xz} + \tau_{yz}\delta\gamma_{yz} \end{pmatrix} dV \tag{11}$$

By substituting Eqs. (5) and (7) into Eq. (11) and integrating the result, the strain energy can be rewritten as

$$\begin{aligned}\delta U_P = \int_A \{ & N_{xx}\delta\varepsilon_{xx}^0 + N_{yy}\delta\varepsilon_{yy}^0 + N_{xy}\delta\gamma_{xy}^0 + M_{xx}^b\delta\kappa_{xx}^b + M_{yy}^b\delta\kappa_{yy}^b + M_{xy}^b\delta\kappa_{xy}^b \\ & + M_{xx}^s\delta\kappa_{xx}^s + M_{yy}^s\delta\kappa_{yy}^s + M_{xy}^s\delta\kappa_{xy}^s + Q_{xz}^s\delta\gamma_{xz}^s + Q_{yz}^s\delta\gamma_{yz}^s \}\, dxdy\end{aligned} \tag{12}$$

where N_{ij}, M_{ij}^b, M_{ij}^s and Q_{ij}^s are the stress resultants defined by

$$\begin{aligned}
\left(N_{xx}, N_{yy}, N_{xy}\right) &= \int_{-h/2}^{h/2} \left(\sigma_{xx}, \sigma_{yy}, \tau_{xy}\right) dz = \sum_{k=1}^{n} \int_{z_k}^{z_{k+1}} \left(\sigma_{xx}, \sigma_{yy}, \tau_{xy}\right) dz \\
\left(M_{xx}^b, M_{yy}^b, M_{xy}^b\right) &= \int_{-h/2}^{h/2} \left(\sigma_{xx}, \sigma_{yy}, \tau_{xy}\right) z dz = \sum_{k=1}^{n} \int_{z_k}^{z_{k+1}} \left(\sigma_{xx}, \sigma_{yy}, \tau_{xy}\right) z\, dz \\
\left(M_{xx}^s, M_{yy}^s, M_{xy}^s\right) &= \int_{-h/2}^{h/2} \left(\sigma_{xx}, \sigma_{yy}, \tau_{xy}\right) \psi(z) dz = \sum_{k=1}^{n} \int_{z_k}^{z_{k+1}} \left(\sigma_{xx}, \sigma_{yy}, \tau_{xy}\right) \psi(z)\, dz \\
\left\{Q_{xz}^s, Q_{yz}^s\right\} &= \int_{-h/2}^{h/2} \left(g(z)\tau_{xz}, g(z)\tau_{yz}\right) dz = \sum_{k=1}^{n} \int_{z_k}^{z_{k+1}} \left(g(z)\tau_{xz}, g(z)\tau_{yz}\right) dz
\end{aligned} \tag{13}$$

where z_k and z_{k+1} denote the lower and upper z-coordinates of the kth layer ($k = 1 - n$), respectively. Furthermore, by substituting Eq. (8) into Eq. (13) and integrating the result, the stress resultants are obtained as

$$\begin{Bmatrix} (1-\mu\nabla^2)N_{xx} \\ (1-\mu\nabla^2)N_{yy} \\ (1-\mu\nabla^2)N_{xy} \\ (1-\mu\nabla^2)M_{xx}^b \\ (1-\mu\nabla^2)M_{yy}^b \\ (1-\mu\nabla^2)M_{xy}^b \\ (1-\mu\nabla^2)M_{xx}^s \\ (1-\mu\nabla^2)M_{yy}^s \\ (1-\mu\nabla^2)M_{xy}^s \end{Bmatrix} = \begin{bmatrix} A_{11} & A_{12} & A_{16} & B_{11} & B_{12} & B_{16} & B_{11}^s & B_{12}^s & B_{16}^s \\ A_{12} & A_{22} & A_{26} & B_{12} & B_{22} & B_{26} & B_{12}^s & B_{22}^s & B_{26}^s \\ A_{16} & A_{26} & A_{66} & B_{16} & B_{26} & B_{66} & B_{16}^s & B_{26}^s & B_{66}^s \\ B_{11} & B_{12} & B_{16} & D_{11} & D_{12} & D_{16} & D_{11}^s & D_{12}^s & D_{16}^s \\ B_{12} & B_{22} & B_{26} & D_{12} & D_{22} & D_{26} & D_{12}^s & D_{22}^s & D_{26}^s \\ B_{16} & B_{26} & B_{66} & D_{16} & D_{26} & D_{66} & D_{16}^s & D_{26}^s & D_{66}^s \\ B_{11}^s & B_{12}^s & B_{16}^s & D_{11}^s & D_{12}^s & D_{16}^s & H_{11}^s & H_{12}^s & H_{16}^s \\ B_{12}^s & B_{22}^s & B_{26}^s & D_{12}^s & D_{22}^s & D_{26}^s & H_{12}^s & H_{22}^s & H_{26}^s \\ B_{16}^s & B_{26}^s & B_{66}^s & D_{16}^s & D_{26}^s & D_{66}^s & H_{16}^s & H_{26}^s & H_{66}^s \end{bmatrix} \begin{Bmatrix} \varepsilon_{xx}^0 \\ \varepsilon_{yy}^0 \\ \gamma_{xy}^0 \\ \kappa_{xx}^b \\ \kappa_{yy}^b \\ \kappa_{xy}^b \\ \kappa_{xx}^s \\ \kappa_{yy}^s \\ \kappa_{xy}^s \end{Bmatrix} \tag{14}$$

$$\begin{bmatrix} (1-\mu\nabla^2)Q_{yz}^s \\ (1-\mu\nabla^2)Q_{xz}^s \end{bmatrix} = \begin{bmatrix} A_{44}^s & A_{45}^s \\ A_{45}^s & A_{55}^s \end{bmatrix} \begin{Bmatrix} \gamma_{yz}^s \\ \gamma_{xz}^s \end{Bmatrix} \tag{15}$$

in which the constitutive stiffness coefficients are given by

$$\begin{aligned}
\left(A_{ij}, B_{ij}, D_{ij}\right) &= \int_{-h/2}^{h/2} \bar{Q}_{ij}\left(1, z, z^2\right) dz \\
\left(B_{ij}^s, D_{ij}^s, H_{ij}^s, A_{ij}^s\right) &= \int_{-h/2}^{h/2} \bar{Q}_{ij}\left(\psi(z), z\psi(z), \psi^2(z), g^2(z)\right) dz
\end{aligned} \tag{16}$$

3.2.2 Energy associated with the elastic foundation

Second, the energy associated with the elastic foundation can be defined as

$$U_F = -\int_A \int_{-h/2}^{h/2} \{U_{\text{Pasternak}}\} dz dA = -\left(q_{\text{Pasternak}}\right) \tag{17}$$

The Pasternak model foundation is a two-parameter elastic model, which consists of a shear layer parameter with stiffness K_P (physically, this parameter is related to the shearing part) and a spring with stiffness K_W (Winkler model). Thus the distributed reaction between the Pasternak foundation and the laminated composite plate can be expressed by (Shahsavari *et al*. 2018d)

$$q_{\text{Pasternak}} = K_{\text{w}}\left(w_b + w_s\right) - K_{\text{p}}\nabla^2\left(w_b + w_s\right) \tag{18}$$

It is clear that the Pasternak model reduces to the Winkler foundation model when $K_P = 0$.

3.2.3 External work

The load potential or work done by external forces is given by

$$\begin{aligned}\delta V = & -\frac{1}{2}\int_A \delta\left[N_{xx}^0\left(\frac{\partial w}{\partial x}\right)^2 + 2N_{xy}^0\frac{\partial w}{\partial x}\frac{\partial w}{\partial y} + N_{yy}^0\left(\frac{\partial w}{\partial y}\right)^2\right] dA \\ & -\int_A qw dA\end{aligned} \tag{19}$$

where N_{xx}^0, N_{yy}^0, and N_{xy}^0 are axial compressive and in-plane shear loads, and q is the distributed transverse force induced by the in-plane magnetic field, which will be defined below

3.2.4 Classical Maxwell's equations

Based on the classical form of Maxwell equations (Narendar *et al*. 2012, Gopalakrishnan and Narendar 2013), the basic relations among the current density **J**, the strength of the electric field **e**, the magnetic field **h** and the magnetic permeability η are

$$\mathbf{J} = \nabla\times\mathbf{h}, \nabla\times\mathbf{e} = -\eta\frac{\partial\mathbf{h}}{\partial\mathrm{t}}, \nabla\cdot\mathbf{h} = 0 \tag{20}$$

where the strengths of the magnetic and electric fields are defined as

$$\mathbf{h} = \nabla\times\left(\mathbf{U}\times\mathbf{H}\right), \mathbf{e} = -\eta\left(\frac{\partial\mathbf{U}}{\partial\mathrm{t}}\times\mathbf{H}\right) \tag{21}$$

in which ∇ is Hamilton operator (vector) in the Cartesian coordinate, $\mathbf{U} = (u, v, w)$ denotes the displacement vector and $\mathbf{H} = (H_x, 0, 0)$ is the given magnetic field vector. In this article, this vector is assumed to be within the laminated composite plate along the x-direction. Thus, we can rewrite the vector of the magnetic field as

$$\mathbf{h} = -H_x\left(\frac{\partial \mathrm{v}}{\partial y} + \frac{\partial \mathrm{w}}{\partial z}\right)\mathbf{i} + H_x\frac{\partial v}{\partial x}\mathbf{j} + H_x\frac{\partial w}{\partial x}\mathbf{k} \tag{22}$$

Substituting Eq. (22) to the first expressions of Eq. (20) yields

$$\begin{aligned}\mathbf{J} = \nabla\times\mathbf{h} = H_x&\left(-\frac{\partial^2 v}{\partial x\,\partial z} + \frac{\partial^2 w}{\partial x\,\partial y}\right)\mathbf{i}\\ -H_x&\left(\frac{\partial^2 v}{\partial y\,\partial z} + \frac{\partial^2 w}{\partial x^2} + \frac{\partial^2 w}{\partial z^2}\right)\mathbf{j}\\ +H_x&\left(\frac{\partial^2 v}{\partial x^2} + \frac{\partial^2 v}{\partial y^2} + \frac{\partial^2 w}{\partial y\,\partial z}\right)\mathbf{k}\end{aligned} \tag{23}$$

Moreover, substituting Eq. (23) into the expressions for the Lorentz force (induced by the in-plane uniaxial magnetic field), one obtains

$$\begin{aligned}\mathbf{f} = f_x\mathbf{i} + f_y\mathbf{j} + f_z\mathbf{k} = \eta(\mathbf{J?}\quad) = \eta\Bigg[0\mathbf{i} + H_x^2&\left(\frac{\partial^2 v}{\partial \mathrm{x}^2} + \frac{\partial^2 v}{\partial \mathrm{y}^2} + \frac{\partial^2 w}{\partial \mathrm{z}\,\partial \mathrm{y}}\right)\mathbf{j}\\ +H_x^2\left(\frac{\partial^2 v}{\partial \mathrm{z}\,\partial \mathrm{y}} + \frac{\partial^2 w}{\partial \mathrm{x}^2} + \frac{\partial^2 w}{\partial \mathrm{z}^2}\right)\mathbf{k}\Bigg]&\end{aligned} \tag{24}$$

in which f_x, f_y and f_z are the Lorentz forces along x, y and z directions, respectively, and in our case they are

$$\begin{aligned}f_x &= 0, f_y = \eta H_x^2\left(\frac{\partial^2 v}{\partial x^2} + \frac{\partial^2 v}{\partial y^2} + \frac{\partial^2 w}{\partial z\,\partial y}\right)\\ f_z &= \eta H_x^2\left(\frac{\partial^2 v}{\partial z\,\partial y} + \frac{\partial^2 w}{\partial x^2} + \frac{\partial^2 w}{\partial z^2}\right)\end{aligned} \tag{25}$$

In this article, we assume that the displacement of laminated composite plates w (x, y, z) and Lorentz force act only in z-direction (Kiani 2014)

$$f_z = \eta H_x^2\left(\frac{\partial^2 v}{\partial z\,\partial y} + \frac{\partial^2 w}{\partial x^2} + \frac{\partial^2 w}{\partial z^2}\right) \tag{26}$$

Accordingly, it is possible to obtain the external Lorentz magnetic force (Wang *et al*. 2012, Karami and Janghorban 2016, Jalaei and Arani 2018), which acts on the laminated composite plates. Based on the displacement field of refined-hyperbolic-shear-deformation-plate theory Eq. (3), we have

$$\begin{aligned}&q_{\text{Lorentz}}(x, y, t) = \int_{-h/2}^{h/2} f_z dz =\\ &\eta h H_x^2\left(\frac{\partial^2 w_b}{\partial x^2} + \frac{\partial^2 w_s}{\partial x^2} - \frac{\partial^2 w_b}{\partial y^2} - 0.165684\frac{\partial^2 w_s}{\partial y^2}\right)\end{aligned} \tag{27}$$

3.3 Equilibrium equations in terms of displacements

For the laminated composite plate thickness in each layer is equal and the equations of motion can be written by substituting the expressions for δU_P, δU_F and δV from Eqs. (12), (17), and (19) into Eq. (10), and integrating, and collecting the coefficients of δu_0, δv_0, δw_b and δw_s which are listed below

$$\delta u_0: \frac{\partial N_{xx}}{\partial x} + \frac{\partial N_{xy}}{\partial y} = 0 \tag{28}$$

$$\delta v_0: \frac{\partial N_{xy}}{\partial x} + \frac{\partial N_{yy}}{\partial y} = 0 \tag{29}$$

$$\begin{aligned}&\delta w_b: \left[\frac{\partial^2 M_{xx}^b}{\partial x^2} + 2\frac{\partial^2 M_{xy}^b}{\partial x\partial y} + \frac{\partial^2 M_{yy}^b}{\partial y^2}\right]\\ &+\left(1-\mu\nabla^2\right)\left(q_{\text{Lorentz}} + N(w) - q_{\text{Pasternak}}\right) = 0\end{aligned} \tag{30}$$

$$\begin{aligned}&\delta w_s: \left[\frac{\partial^2 M_{xx}^s}{\partial x^2} + 2\frac{\partial^2 M_{xy}^s}{\partial x\partial y} + \frac{\partial^2 M_{yy}^s}{\partial y^2} + \frac{\partial Q_{xz}^s}{\partial x} + \frac{\partial Q_{yz}^s}{\partial y}\right]\\ &+\left(1-\mu\nabla^2\right)\left(q_{\text{Lorentz}} + N(w) - q_{\text{Pasternak}}\right) = 0\end{aligned} \tag{31}$$

By substituting Eqs. (14), (15), (18), (19) and (27) into Eqs. (28)-(32), the equations of motion for the nonlocal laminated composite plate can be expressed in terms of displacements (u_0, v_0, w_b, w_s) as follow

$$\begin{aligned}&\left[A_{11}d_{11} + 2A_{16}d_{12} + A_{66}d_{22}\right]u_0\\ &+\left[A_{16}d_{11} + \left(A_{12} + A_{66}\right)d_{12} + A_{26}d_{22}\right]v_0\\ &-\left[B_{11}d_{111} + 3B_{16}d_{112} + \left(B_{12} + 2B_{66}\right)d_{122} + B_{26}d_{222}\right]w_b\\ &-\left[B_{11}^s d_{111} + 3B_{16}^s d_{112} + \left(B_{12}^s + 2B_{66}^s\right)d_{122} + B_{26}^s d_{222}\right]w_s = 0\end{aligned} \tag{32}$$

$$\begin{aligned}&\left[A_{16}d_{11} + \left(A_{12} + A_{66}\right)d_{12} + A_{26}d_{22}\right]u_0\\ &+\left[A_{66}d_{11} + 2A_{26}d_{12} + A_{22}d_{22}\right]v_0\\ &-\left[B_{16}d_{111} + \left(B_{12} + 2B_{66}\right)d_{112} + 3B_{26}d_{122} + B_{22}d_{222}\right]w_b\\ &-\left[B_{16}^s d_{111} + \left(B_{12}^s + 2B_{66}^s\right)d_{112} + 3B_{26}^s d_{122} + B_{22}^s d_{222}\right]w_s = 0\end{aligned} \tag{33}$$

$$\begin{aligned}&\left[B_{11}d_{111} + 3B_{16}d_{112} + \left(B_{12} + 2B_{66}\right)d_{122} + B_{26}d_{222}\right]u_0\\ &+\left[B_{16}d_{111} + \left(B_{12} + 2B_{66}\right)d_{112} + 3B_{26}d_{122} + B_{22}d_{222}\right]v_0\\ &-\left[D_{11}d_{1111} + 4D_{16}d_{1112} + 2\left(D_{12} + 2D_{66}\right)d_{1122} + 4D_{26}d_{1222} + D_{22}d_{2222}\right]w_b\\ &-\left[D_{11}^s d_{1111} + 4D_{16}^s d_{1112} + 2\left(D_{12}^s + 2D_{66}^s\right)d_{1122} + 4D_{26}^s d_{1222} + D_{22}^s d_{2222}\right]w_s\\ &+\Bigg[\eta h H_x^2\left\{\left(d_{11} + d_{22}\right) - \mu\left(d_{1111} + 2d_{1122} + d_{2222}\right)\right\}\\ &-\underbrace{(\underbrace{K_w\left\{1-\mu\left(d_{11} + d_{22}\right)\right\}}_{q_{\text{winkler}}} - K_p\left\{\left(d_{11} + d_{22}\right) - \mu\left(d_{1111} + 2d_{1122} + d_{2222}\right)\right\})}_{q_{\text{Pasternak}}}\Bigg]\left(w_b + w_s\right)\\ &+\Big[N_{xx}^0\left\{d_{11} - \mu\left(d_{1111} + d_{1122}\right)\right\} + 2N_{xy}^0\left\{d_{12} - \mu\left(d_{1112} + d_{1222}\right)\right\}\\ &+N_{yy}^0\left\{d_{22} - \mu\left(d_{1122} + d_{2222}\right)\right\}\Big]\left(w_b + w_s\right) = 0\end{aligned} \tag{34}$$

$$
\begin{aligned}
&\left[B_{11}^{s} d_{111}+3 B_{16}^{s} d_{112}+\left(B_{12}^{s}+2 B_{66}^{s}\right) d_{122}+B_{26}^{s} d_{222}\right] u_{0} \\
&+\left[B_{16}^{s} d_{111}+\left(B_{12}^{s}+2 B_{66}^{s}\right) d_{112}+3 B_{26}^{s} d_{122}+B_{22}^{s} d_{222}\right] v_{0} \\
&-\left[D_{11}^{s} d_{1111}+4 D_{16}^{s} d_{1112}+2\left(D_{12}^{s}+2 D_{66}^{s}\right) d_{1122}+4 D_{26}^{s} d_{1222}+D_{22}^{s} d_{2222}\right] w_{b} \\
&-\left[H_{11}^{s} d_{1111}+4 H_{16}^{s} d_{1112}+2\left(H_{12}^{s}+2 H_{66}^{s}\right) d_{1122}+4 H_{26}^{s} d_{1222}+H_{22}^{s} d_{2222}\right. \\
&\left.-A_{55}^{s} d_{11}-A_{44}^{s} d_{22}-2 A_{45}^{s} d_{12}\right] w_{s}+\Big[\eta h H_{x}^{2}\left\{\left(d_{11}+d_{22}\right)-\mu\left(d_{1111}+2 d_{1122}+d_{2222}\right)\right\} \\
&\left.-\underbrace{(\underbrace{K_{w}\left\{1-\mu\left(d_{11}+d_{22}\right)\right\}}_{q_{\text{winkler}}}-K_{p}\left\{\left(d_{11}+d_{22}\right)-\mu\left(d_{1111}+2 d_{1122}+d_{2222}\right)\right\})}_{q_{\text{Pasternak}}}\right]\left(w_{b}+w_{s}\right) \\
&+\left[N_{xx}^{0}\left\{d_{11}-\mu\left(d_{1111}+d_{1122}\right)\right\}+2 N_{xy}^{0}\left\{d_{12}-\mu\left(d_{1112}+d_{1222}\right)\right\}\right. \\
&\left.+N_{yy}^{0}\left\{d_{22}-\mu\left(d_{1122}+d_{2222}\right)\right\}\right]\left(w_{b}+w_{s}\right)=0
\end{aligned} \tag{35}
$$

In which d_{ij}, d_{ijk} and d_{ijkl} denote the differential operators defined below

$$
\begin{aligned}
& d_{ij}=\frac{\partial^{2}}{\partial x_{i} x_{j}}, d_{ijk}=\frac{\partial^{3}}{\partial x_{i} x_{j} x_{k}} \\
& d_{ijkl}=\frac{\partial^{4}}{\partial x_{i} x_{j} x_{k} x_{l}} ;\{i, j, k, l=1,2\}
\end{aligned} \tag{36}
$$

4. Closed-form solution of laminated composite plates

A rectangular plate with length a and width b under the magnetic field and in-plane loads is shown in Fig. 2.

The Navier solution can be developed for the rectangular laminated plate under simply supported boundary conditions. In this study, two types of simply supported (SS) (SS-1, SS-2) boundary conditions for the rectangular laminated plate under magnetic field along the x-axis (H_x, 0, 0) and in-plane loads in x- and y-directions ($N_x^0 \equiv \lambda N,\ N_y^0 \equiv \gamma N$) are considered, as discussed below.

4.1 Analytical solutions for antisymmetric cross-ply laminates under boundary condition SS-1

For this case, the following plate stiffness elements are identically zero

$$
\begin{aligned}
& A_{16}=A_{26}=D_{16}=D_{26}=D_{16}^{s}=D_{26}^{s}=H_{16}^{s}=H_{26}^{s}=0 \\
& B_{12}=B_{16}=B_{26}=B_{66}=B_{12}^{s}=B_{16}^{s}=B_{26}^{s}=B_{66}^{s}=A_{45} \\
& =A_{45}^{s}=D_{45}=0, B_{22}=-B_{11}=B_{22}^{s}=-B_{11}^{s},
\end{aligned} \tag{37}
$$

The following SS-1 boundary conditions are imposed at the edges:

1. On edges $x = 0$, a:

$$\left\{v_{0}, w_{b}, w_{s}, \partial w_{b} / \partial y, \partial w_{s} / \partial y, N_{xx}, M_{xx}^{b}, M_{xx}^{s}\right\}=0 \tag{38}$$

2. On edges $y = 0$, b:

$$\left\{u_{0}, w_{b}, w_{s}, \partial w_{b} / \partial x, \partial w_{s} / \partial x, N_{yy}, M_{yy}^{b}, M_{yy}^{s}\right\}=0 \tag{39}$$

Following the Navier solution method and considering the boundary condition Eqs. (38)-(39), the solutions of the displacements $u_0(x, y)$, $v_0(x, y)$, $w_b(x, y)$, and $w_s(x, y)$ that satisfy the boundary conditions exactly can be assumed as

$$
\left\{\begin{array}{l}
u_{0} \\
v_{0} \\
w_{b} \\
w_{s}
\end{array}\right\}=\sum_{m=1}^{\infty} \sum_{n=1}^{\infty}\left\{\begin{array}{l}
U_{mn} \cos (\alpha x) \sin (\beta y) e^{i \omega t} \\
V_{mn} \sin (\alpha x) \cos (\beta y) e^{i \omega t} \\
W_{bmn} \sin (\alpha x) \sin (\beta y) e^{i \omega t} \\
W_{smn} \sin (\alpha x) \sin (\beta y) e^{i \omega t}
\end{array}\right\} \tag{40}
$$

where ω is the eigen-frequency associated with the (m,n)-th eigen-mode, and $\alpha = m\pi/a$, $\beta = n\pi/b$. Also, U_{mn}, V_{mn}, W_{bmn}, and W_{smn} are four unknown coefficients to be determined, which form the amplitude vector.

4.2 Analytical solutions for antisymmetric angle-ply laminates under boundary condition SS-2

For this case, the following plate stiffness elements are identically zero

$$
\begin{aligned}
& A_{16}=A_{26}=D_{16}=D_{26}=D_{16}^{s}=D_{26}^{s}=H_{16}^{s}=H_{26}^{s}=0 \\
& B_{12}=B_{16}=B_{26}=B_{66}=B_{12}^{s}=B_{16}^{s}=B_{26}^{s}=B_{66}^{s}=0 \\
& A_{45}=A_{45}^{s}=D_{45}=0
\end{aligned} \tag{41}
$$

The following SS-2 boundary conditions are imposed at the edges:

1. On edges $x = 0$, a:

$$\left\{u_{0}, w_{b}, w_{s}, \partial w_{b} / \partial y, \partial w_{s} / \partial y, N_{xy}, M_{xx}^{b}, M_{xx}^{s}\right\}=0 \tag{42}$$

2. On edges $y = 0$, b:

$$\left\{v_{0}, w_{b}, w_{s}, w_{e}, \partial w_{b} / \partial x, \partial w_{s} / \partial x, \partial w_{e} / \partial x, N_{xy}, M_{yy}^{b}, M_{yy}^{s}\right\}=0 \tag{43}$$

Similar to the cross-ply laminate case, the solutions of the displacements which satisfy the boundary conditions exactly can be assumed as

$$
\left\{\begin{array}{l}
u_{0} \\
v_{0} \\
w_{b} \\
w_{s}
\end{array}\right\}=\sum_{m=1}^{\infty} \sum_{n=1}^{\infty}\left\{\begin{array}{l}
U_{mn} \sin (\alpha x) \cos (\beta y) e^{i \omega t} \\
V_{mn} \cos (\alpha x) \sin (\beta y) e^{i \omega t} \\
W_{bmn} \sin (\alpha x) \sin (\beta y) e^{i \omega t} \\
W_{smn} \sin (\alpha x) \sin (\beta y) e^{i \omega t}
\end{array}\right\} \tag{44}
$$

4.3 Eigenvalue problem for buckling problems

By substituting Eq. (40) or Eq. (44) into Eqs. (32)-(35), we obtain the following eigenvalue equations

$$([K]-[P])\{\Delta\}=\{0\} \tag{45}$$

where $[K]$, $[P]$, and $\{\Delta\}$ are the stiffness matrix, applied force matrix, and the unknown amplitude vector, respectively.

Table 1 Material properties of the laminated composite plates

Type	E_2 (GPa)	E_1	G_{12}	G_{13}	G_{23}	ν_{12}
1[a]	1	(3,10,20,30,40)E_2	0.6E_2	0.6E_2	0.5E_2	0.25
2[b]	1	25E_2	0.5E_2	0.5E_2	0.2E_2	0.25

[a] (Noor 1975); [b] (Phan and Reddy 1985)

Table 2 Normalized uniaxial critical buckling load $\widehat{N}$ of simply supported isotropic nanobeam with $\lambda = 1$, $\gamma = 0$, $a = 10$ nm, $b = \rightarrow \infty$, $E_1 = E_2 = 30$(MPa), and $\nu_{12} = \nu_{21} = 0.3$

a/h	μ (nm^2)	NFSDT (k = 2/3)*a	NHSDT[b]	NTVRPT[a]	Present
20	0	9.8005	9.8067	9.8067	9.8005
	1	8.9466	8.9528	8.9528	8.9201
	2	8.1838	8.1900	8.1900	8.1849
100	0	9.8668	9.8671	9.8671	9.8668
	1	8.9804	8.9807	8.9807	8.9805
	2	8.2402	8.2405	8.2405	8.2403

[a] (Narendar 2011); [b] (Pradhan 2009)

5. Numerical results

In this section, various numerical examples are presented to show the accuracy of the refined-hyperbolic-shear-deformation-plate theory and the behavior of buckling of laminated composite plates rested on the elastic Pasternak foundation with and without the nonlocal parameter. The plate is under the in-plane magnetic field as well as in-plane mechanical loads. In these examples, the effects of several parameters such as nonlocal parameter, magnetic field, foundation parameters, moduli ratio, thickness ratio, length-to-width ratio, lay-up numbers, fiber orientations, symmetric or antisymmetric lay-up of layers, eigenmodes m and n and various coupled conditions on the critical buckling load are investigated. To present the numerical results and compared some of them with existing ones, the following non-dimensional and dimensional parameters are introduced (Kim *et al*. 2009, Thai and Kim 2010, Murmu *et al*. 2013)

$$\hat{N} = \frac{Na^2}{D_0}, \tilde{N} = \frac{Na^2}{E_2 h^3}, \mathrm{MP} = \frac{\eta h H_x^2 a^2}{D_0},$$
$$\bar{K}_W = \frac{K_W a^4}{E_2 h^3}, \bar{K}_P = \frac{K_P a^2}{E_2 h^3}, G = \frac{E_1}{2(1+\nu_{12})}$$
$$D_0 = \frac{E_2 h^3}{12(1-\nu_{12}\nu_{21})}$$

Two types of laminated composite plates are employed in this study. In Table 1, these material properties are listed. In all examples, the length of the laminated composite plate is fixed.

5.1 Validation

The nonlocal buckling of laminated composite plates is developed for the first time in the present work. Hence, the results are obtained and compared with available ones in the literature to validate the present nonlocal refined-hyperbolic-shear-deformable plate theory. Table 2 lists the critical buckling loads of nonlocal isotropic beam using the present formulation, as compared to those based on the theories of nonlocal first-order-shear-deformation theory (NFSDT) (Narendar 2011), nonlocal higher-order-shear-deformation theory (NHSDT) (Pradhan 2009), and nonlocal two-variable-refined-plate theory (NTVRPT) (Narendar 2011). As it is shown, the present results are in excellent agreement with those reported by Narendar (2011) and Pradhan (2009).

5.2 Buckling analysis

Let us consider a rectangular and simply supported laminated composite plate with length a, width b, and thickness h, which is surrounded by a Pasternak foundation and subjected to an in-plane magnetic field. Also uniform compressive edge loads of magnitude (λN) along x-direction and (γN) along y-direction of the plate as shown in Fig. 2 are also applied with $N_{xx}^0 = \lambda N,\ N_{yy}^0 = \gamma N,\ N_{xy}^0 = 0$ in Eqs. (34)-(35).

5.2.1 Effect of moduli ratios and elastic foundations

In Table 3, the uniaxial and biaxial critical buckling loads of a cross-ply [0/90/0] laminated plate made of Material 1 is first presented for different moduli ratios as compared with various methods (Reddy 2004, Singh *et al*. 2013). It is observed that the present results are acceptable for different values of moduli ratio (E_1/E_2 = 3, 10, 20, 30) even when compared with analytical results of Reddy (Reddy 2004) and meshless method (Singh *et al*. 2013), except for the high moduli ratio case. As it is observed, the buckling loads for the case of uniaxial compression are always higher than the corresponding biaxial ones. Listed in Table 3 is also the influence of the size effect and elastic foundation on the uniaxial and biaxial critical buckling loads of the laminated plate. It is seen that with increasing nonlocal parameter, the laminated plate structure becomes more flexible, resulting in a reduced buckling load under a constant foundation stiffness. This is due to the fact that with increasing nonlocal parameter, the interaction forces between atoms of structure will decrease and thus the laminated plate becomes softer. However, the difference between nonlocal and local results decreases with increasing spring constant and shear layer parameter of the elastic foundation. It is also observed from Table 3, that existence of an elastic foundation would increase the buckling load of the laminated composite plates. This is reasonable since a composite plate on the foundation is stiffer than that without foundation. Moreover, when the laminated plate rests on the Pasternak foundation ($\bar{K}_W \neq 0,\ \bar{K}_P \neq 0$), the stiffness of the system due to an extra shear layer increases, and consequently, leads to the increase in bending rigidity and buckling load of the structure.

Table 3 Normalized uniaxial and biaxial critical buckling load $\tilde{N}$ of a symmetrically laminated composite plate resting on elastic foundations with different moduli ratio, and nonlocal parameter, (layup [0/90/0] of Material 1, a/h = 100, for uniaxial: λ = 1, γ = 0, for biaxial: λ = 1, γ = 1)

Load type	$\bar{K}_W$	$\bar{K}_P$	μ	Method	E_1/E_2			
					3	10	20	30
Uniaxial	0	0	0	Reddy[(a)]	5.7540	11.4920	19.7120	27.9360
				Meshless Method[(b)]	5.7580	11.4880	19.6741	27.8366
				Present	5.7502	11.4774	19.6701	27.8508
			1	Present	4.8022	9.5853	16.4274	23.2596
			2	Present	4.1226	8.2288	14.1026	19.9679
	100	0	0	Present	15.8823	21.6095	29.8022	37.9830
			1	Present	14.9344	19.7174	26.5596	33.3917
			2	Present	14.2547	18.3609	24.2347	30.1000
		10	0	Present	35.8823	41.6095	49.8022	57.9830
			1	Present	34.9344	39.7174	46.5596	53.3917
			2	Present	34.2547	38.3609	44.2347	50.1000
Biaxial	0	0	0	Reddy[(a)]	–	5.7460	9.5910	12.1470
				Meshless Method[(b)]	2.8790	5.7441	9.5659	12.0962
				Present	2.8751	5.7387	9.8351	13.9254
			1	Present	2.4011	4.7927	8.2137	11.6298
			2	Present	2.0613	4.1144	7.0513	9.9839
	100	0	0	Present	7.9411	10.8048	14.9011	18.9915
			1	Present	7.4672	9.8587	13.2798	16.6959
			2	Present	7.1274	9.1805	12.1174	15.0500
		10	0	Present	17.9411	20.8048	24.9011	28.9915
			1	Present	17.4672	19.8587	23.2798	26.6959
			2	Present	17.1274	19.1805	22.1174	25.0500

[(a)] (Reddy 2004); [(b)] (hpg *et al*. 2013)

5.2.2 Effect of thickness ratios and magnetic field

The uniaxial buckling loads of the cross-ply [0/90] and angle-ply [45/-45] laminated plates with two layers for various values of thickness ratio (a/h = 10, 20, 50, 100) are presented in Table 4. The results obtained by different methods (Mixed Interpolation Smoothing Quadrilateral element with 24 DOFs (MISQ24), First-order Shear Deformation Theory (FSDT) using Finite Element Method (FEM) to solve the problem, and Higher-Order Shear Deformation Theory (HSDT)) (Nguyen-Van *et al*. 2011, Chakrabarti and Sheikh 2003, Reddy and Phan 1985) are also listed for comparison. It is easy to see that the present results are in good agreement with those reported in references (Nguyen-Van *et al*. 2011, Chakrabarti and Sheikh 2003, Reddy and Phan 1985) for all the cases ranging from very thin to moderately thick plates. It is further observed from the present results that increasing the nonlocal parameter (magnetic field) will lead to a/an decrease (increase) in buckling loads, respectively. Moreover, it is also concluded that for both of cross-ply and angle-ply laminated plate with two layers, the nonlocal parameter and magnetic field will influence more the buckling loads for small values of the thickness ratios.

5.2.3 Effect of the lay-up numbers and fiber orientations

In Fig. 3, uniaxial buckling loads of the square antisymmetric laminated plates with two, four and ten layers of angle-ply composite plates are presented to illustrate the effects of the nonlocal parameter as well as the variation of fiber orientations (ply-angle) from 0-90. As it can be seen, in the laminated composite plate with increasing number of layers, the buckling load will increase. For fixed lay-up numbers and if the composite plate is made of two antisymmetric layers, the maximum buckling loads will occur when ply-angles equal to 0 and 90; however, if the plate is made of more than two layers, the maximum buckling load will occur at ply-angle $\approx$ 45. Besides, an increment in nonlocal parameter is proportional to the decrement in the peak value of buckling load.

Table 4 Normalized uniaxial critical buckling load $\tilde{N}$ of cross-ply and angle-ply square laminated composite plates with various values of thickness ratio, magnetic field (MP) and nonlocal parameter, (λ = 1, γ = 0, for cross-ply: Material 1 with [0/90], E_1/E_2 = 40 and SS-1 and for angle-ply: Material 2 with [45/-45] and SS-2)

	MP	μ	Method	a/h = 10	20	50	100
Cross-ply	0	0	MISQ24[*a]	11.360	12.551	12.906	13.039
			FSDT[*b]	11.349	12.510	12.879	12.934
			HSDT[*c]	11.563	12.577	12.895	12.943
			Present	11.560	12.576	12.895	12.942
		1	Present	9.654	10.503	10.769	10.808
		2	Present	8.288	9.0167	9.245	9.279
	50	0	Present	11.965	12.632	12.898	12.942
		1	Present	10.140	10.569	10.773	10.809
		2	Present	8.854	9.094	9.250	9.279
	100	0	Present	12.371	12.687	12.902	12.943
		1	Present	10.625	10.635	10.778	10.809
		2	Present	9.419	9.171	9.255	9.280
Angle-ply	0	0	MISQ24[*a]	12.042	14.500	15.374	15.510
			FSDT[*b]	12.600	14.629	15.329	15.435
			HSDT[*c]	12.622	14.644	15.336	15.441
			Present	12.617	14.642	15.336	15.441
		1	Present	10.537	12.229	12.808	12.895
		2	Present	9.046	10.498	10.995	11.070
	50	0	Present	13.311	14.744	15.343	15.441
		1	Present	11.366	12.350	12.816	12.896
		2	Present	10.014	10.639	11.005	11.071
	100	0	Present	14.006	14.845	15.349	15.442
		1	Present	12.200	12.471	12.824	12.897
		2	Present	10.983	10.780	11.014	11.073

[(a)] (Nguyen-Van *et al*. 2011); [(b)] (Chakrabarti and Sheikh 2003); [(c)] (Reddy and Phan 1985)

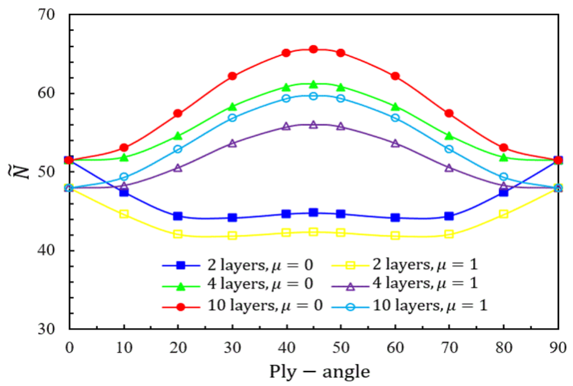

Fig. 3 The variation of uniaxial critical buckling load $\tilde{N}$ vs fiber orientations (ply-angle) of the square antisymmetric laminated composite plate resting on elastic foundation with different values of the nonlocal parameter and lay-up numbers (number of layers), (Material 2 with a/b = 10 and SS-2, λ = 1, γ = 0, $\bar{K}_W$ = 100, $\bar{K}_P$ = 10)

5.2.4 Effect of different lay-ups of layers

We now study the effect of different lay-ups of layers on the uniaxial and biaxial buckling of laminated composite plates resting on Pasternak foundation with various nonlocal parameters, magnetic parameters, and aspect ratio. Listed in Table 5 are the normalized critical buckling loads of four-layer symmetric [0/90/90/0] and antisymmetric [0/90/0/90] cross-plies laminated composite plates subjected to buckling loads in *x*-, or *y*-direction (uniaxial compression) and in both directions (biaxial compressions). It is noted: (1) for the square composite plate (a = b), the critical buckling loads are the same by the uniaxial buckling compression in either *x*- or *y*-direction due to the fact that the composite plate is still orthotropic for these two types of lay-ups; (2) the critical uniaxial buckling load, regardless of its compression direction, is always larger than that under biaxial compressions; (3) the critical uniaxial buckling load in *x*-direction increases with increasing aspect ratio a/b for both lay-ups of the composite plates with fixed magnetic field and fixed nonlocal parameter; (4) under both uniaxial

Table 5 Normalized critical buckling load $\widetilde{N}$ of symmetric and antisymmetric stiff laminated composite plates subjected to uniaxial compression along the *x*-axis (1,0), and *y*-axis (0,1) and biaxial compression (1,1),(a/h = 20, Material 1 with E_1/E_2 = 10 and SS-1; for symmetric: [0/90/90/0] and for antisymmetric: [0/90/0/90], $\bar{K}_W = 100,\ \bar{K}_P = 10$)

			MP = 0			MP = 100		
			Uniaxial (λ, γ)		Biaxial (λ, γ)	Uniaxial (λ, γ)		Biaxial (λ, γ)
Arrangement	a/b	μ	(1,0)	(0,1)	(1,1)	(1,0)	(0,1)	(1,1)
Symmetric	0.5	0	30.413	121.653	24.331	33.588	134.352	26.870
		1	29.559	118.235	23.647	33.125	132.500	26.500
		2	28.873	115.493	23.099	32.831	131.325	26.265
	1	0	41.275	41.275	20.637	41.381	41.381	20.691
		1	39.438	39.438	19.719	39.565	39.565	19.783
		2	38.121	38.121	19.061	38.269	38.269	19.135
Antisymmetric	0.5	0	27.343	109.371	21.874	30.506	122.023	24.405
		1	26.825	107.302	21.460	30.379	121.514	24.303
		2	26.411	105.642	21.128	30.354	121.415	24.283
	1	0	40.139	40.139	20.069	40.235	40.235	20.118
		1	38.489	38.489	19.245	38.605	38.605	19.302
		2	37.306	37.306	18.653	37.441	37.441	18.721

and biaxial buckling loads and for cross-ply symmetric and antisymmetric laminated plates, the critical buckling loads increase with increasing magnetic field (MP) and increase with decreasing nonlocal parameter; (5) In the case of high magnetic field, the size effects has a minor role on the buckling responses, so, the imposed magnetic field is a key parameter for critical buckling controlling of the laminated composite plates.

6. Conclusions

The uniaxial and biaxial buckling loads of the symmetric and antisymmetric laminated composite plates resting on the Pasternak elastic foundation and subjected to the in-plane magnetic field are studied considering nonlocal effect. The equations of motion are derived based on the novel refined-hyperbolic-shear-deformation-plate theory combined with the nonlocal elasticity theory. Both the cross-ply and angle-ply laminated plates under two kinds of simply supported lateral boundary conditions (namely, SS-1 and SS-2), are examined. The expressions for the buckling loads of the laminated composite plates are derived by applying the Navier solution method. Various numerical examples are carried out to study the influences of the diverse range of parameters on the buckling behavior of the laminated plates. Based on these examples, the following conclusions can be drawn:

- The results obtained by the present model with only four variables, are found to be accurate and comparable to those obtained by higher-order-shear-deformation theories which involve more number of unknown variables.
- Unlike the local plate models, the proposed new model can capture the size effects in laminated composite plates.
- For the given material properties and plate geometry, the influence of the applied magnetic field increases monotonically with decreasing thickness ratio.
- When the laminated composite plate is made of an odd number of layers, its critical buckling loads are larger than that made of an even number of layers adjacent to the odd number.

Acknowledgments

We would like to express our great appreciation to Dr. Ernian Pan, Professor of Civil Engineering and Applied Mathematics, University of Akron, OH, USA for his comments and scientific guidance that greatly improved the manuscript.

References

Arefi, M. (2018), “Nonlocal free vibration analysis of a doubly curved piezoelectric nano shell”, *Steel Compos. Struct., Int. J.*, **27**(4), 479-493. https://doi.org/10.12989/scs.2018.27.4.479

Asemi, K. and Shariyat, M. (2016), “Three-dimensional biaxial post-buckling analysis of heterogeneous auxetic rectangular plates on elastic foundations by new criteria”, *Comput. Methods Appl. Mech. Eng.*, **302**, 1-26. https://doi.org/10.1016/j.cma.2015.12.026

Askes, H. and Aifantis, E.C. (2011), “Gradient elasticity in statics and dynamics: an overview of formulations, length scale identification procedures, finite element implementations and new results”, *Int. J. Solids Struct.*, **48**(13), 1962-1990. https://doi.org/10.1016/j.cma.2015.12.026

Aydogdu, M. (2009), “A general nonlocal beam theory: its application to nanobeam bending, buckling and vibration", *Physica E*: *Low-dimens*. *Syst*. *Nanostruct*., **41**(9), 1651-1655. https://doi.org/10.1016/j.physe.2009.05.014

Babuška, I. and Li, L. (1992), "The problem of plate modeling: Theoretical and computational results", *Comput*. *Methods Appl*. *Mech*. *Eng*., **100**(2), 249-273. https://doi.org/10.1016/0045-7825(92)90185-M

Beldjelili, Y., Tounsi, A. and Mahmoud, S. (2016), "Hygro-thermo-mechanical bending of S-FGM plates resting on variable elastic foundations using a four-variable trigonometric plate theory", *Smart Struct*. *Syst*., *Int*. *J*., **18**(4), 755-786. http://dx.doi.org/10.12989/sss.2016.18.4.755

Benachour, A., Tahar, H.D., Atmane, H.A., Tounsi, A. and Ahmed, M.S. (2011), "A four variable refined plate theory for free vibrations of functionally graded plates with arbitrary gradient", *Compos*. *Part B*: *Eng*., **42**(6), 1386-1394. https://doi.org/10.1016/j.compositesb.2011.05.032

Boukhari, A., Atmane, H.A., Tounsi, A., Adda, B. and Mahmoud, S. (2016), "An efficient shear deformation theory for wave propagation of functionally graded material plates", *Struct*. *Eng*. *Mech*., *Int*. *J*., **57**(5), 837-859. http://dx.doi.org/10.12989/sem.2016.57.5.837

Bourada, M., Tounsi, A., Houari, M.S.A. and Bedia, E.A.A. (2012), "A new four-variable refined plate theory for thermal buckling analysis of functionally graded sandwich plates", *J*. *Sandw*. *Struct*. *Mater*., **14**(1), 5-33. https://doi.org/10.1177/1099636211426386

Bousahla, A.A., Benyoucef, S., Tounsi, A. and Mahmoud, S.R. (2016), "On thermal stability of plates with functionally graded coefficient of thermal expansion", *Struct*. *Eng*. *Mech*., *Int*. *J*., **60**(2), 313-335. http://dx.doi.org/10.12989/sem.2016.60.2.313

Chakrabarti, A. and Sheikh, A. (2003), "Buckling of laminated composite plates by a new element based on higher order shear deformation theory", *Mech*. *Adv*. *Mater*. *Struct*., **10**(4), 303-317. https://doi.org/10.1080/10759410306754

Cosserat, E. (1909), F Cosserat Theorie des Corps Deformables Herman and Co., Paris, France.

Eringen, A.C. and Edelen, D. (1972), "On nonlocal elasticity", *Int*. *J*. *Eng*. *Sci*., **10**(3), 233-248. https://doi.org/10.1016/0020-7225(72)90039-0

Farajpour, A., Ghayesh, M.H. and Farokhi, H. (2018), "Large-amplitude coupled scale-dependent behaviour of geometrically imperfect NSGT nanotubes", *Int*. *J*. *Mech*. *Sci*., **150**, 510-525. https://doi.org/10.1016/j.ijmecsci.2018.09.043

Farajpour, A., Farokhi, H. and Ghayesh, M.H. (2019), "Chaotic motion analysis of fluid-conveying viscoelastic nanotubes", *Eur*. *J*. *Mech*.-*A*/*Solids*, **74**, 281-296. https://doi.org/10.1016/j.euromechsol.2018.11.012

Farokhi, H. and Ghayesh, M.H. (2015a), "Nonlinear dynamical behaviour of geometrically imperfect microplates based on modified couple stress theory", *Int*. *J*. *Mech*. *Sci*., **90**, 133-144. https://doi.org/10.1016/j.ijmecsci.2014.11.002

Farokhi, H. and Ghayesh, M.H. (2015b), "Thermo-mechanical dynamics of perfect and imperfect Timoshenko microbeams", *Int*. *J*. *Eng*. *Sci*., **91**, 12-33. https://doi.org/10.1016/j.ijengsci.2015.02.005

Farokhi, H. and Ghayesh, M.H. (2016), "Size-dependent parametric dynamics of imperfect microbeams", *Int*. *J*. *Eng*. *Sci*., **99**, 39-55. https://doi.org/10.1016/j.ijengsci.2015.10.014

Farokhi, H. and Ghayesh, M.H. (2018a), "Nonlinear mechanics of electrically actuated microplates", *Int*. *J*. *Eng*. *Sci*., **123**, 197-213. https://doi.org/10.1016/j.ijengsci.2017.08.017

Farokhi, H. and Ghayesh, M.H. (2018b), "On the dynamics of imperfect shear deformable microplates", *Int*. *J*. *Eng*. *Sci*., **133**, 264-283. https://doi.org/10.1016/j.ijengsci.2018.04.011

Fourn, H., Atmane, H.A., Bourada, M., Bousahla, A.A., Tounsi, A. and Mahmoud, S. (2018), "A novel four variable refined plate theory for wave propagation in functionally graded material plates", *Steel Compos*. *Struct*., *Int*. *J*., **27**(1), 109-122. http://dx.doi.org/10.12989/scs.2018.27.1.109

Ghavanloo, E. and Fazelzadeh, S.A. (2013), "Nonlocal elasticity theory for radial vibration of nanoscale spherical shells", *Eur*. *J*. *Mech*.-*A*/*Solids*, **41**, 37-42. https://doi.org/10.1016/j.euromechsol.2013.02.003

Ghayesh, M.H. (2018), "Mechanics of viscoelastic functionally graded microcantilevers", *Eur*. *J*. *Mech*.-*A*/*Solids*, **73**, 492-499. https://doi.org/10.1016/j.euromechsol.2018.09.001

Ghayesh, M.H., Farokhi, H. and Hussain, S. (2016), "Viscoelastically coupled size-dependent dynamics of microbeams", *Int*. *J*. *Eng*. *Sci*., **109**, 243-255. https://doi.org/10.1016/j.ijengsci.2016.09.004

Ghayesh, M.H., Farokhi, H., Gholipour, A., Hussain, S. and Arjomandi, M. (2017a), "Resonance responses of geometrically imperfect functionally graded extensible microbeams", *J*. *Computat*. *Nonlinear Dyn*., **12**(5), 051002. https://doi.org/10.1115/1.4035214

Ghayesh, M.H., Farokhi, H., Gholipour, A. and Tavallaeinejad, M. (2017b), "Nonlinear bending and forced vibrations of axially functionally graded tapered microbeams", *Int*. *J*. *Eng*. *Sci*., **120**, 51-62. https://doi.org/10.1016/j.ijengsci.2017.03.010

Ghayesh, M.H., Farokhi, H., Gholipour, A. and Tavallaeinejad, M. (2018), "Nonlinear oscillations of functionally graded microplates", *Int*. *J*. *Eng*. *Sci*., **122**, 56-72. ttps://doi.org/10.1016/j.ijengsci.2017.03.014

Gholipour, A., Farokhi, H. and Ghayesh, M.H. (2015), "In-plane and out-of-plane nonlinear size-dependent dynamics of microplates", *Nonlinear Dyn*., **79**(3), 1771-1785. https://doi.org/10.1007/s11071-014-1773-7

Gibson, R.F. (2016), *Principles of Composite Material Mechanics*, CRC press.

Gopalakrishnan, S. and Narendar, S. (2013), *Wave propagation in nanostructures*, Springer, Switzerland.

Hachemi, H., Kaci, A., Houari, M.S.A., Bourada, M., Tounsi, A. and Mahmoud, S. (2017), "A new simple three-unknown shear deformation theory for bending analysis of FG plates resting on elastic foundations", *Steel Compos*. *Struct*., *Int*. *J*., **25**(6), 717-726. http://dx.doi.org/10.12989/scs.2017.25.6.717

Hirwani, C.K., Panda, S.K. and Mahapatra, T.R. (2018), "Thermomechanical deflection and stress responses of delaminated shallow shell structure using higher-order theories", *Compos*. *Struct*., **184**, 135-145. https://doi.org/10.1016/j.compstruct.2017.09.071

Houari, M.S.A., Tounsi, A., Bessaim, A. and Mahmoud, S. (2016), "A new simple three-unknown sinusoidal shear deformation theory for functionally graded plates", *Steel Compos*. *Struct*., *Int*. *J*., **22**(2), 257-276. https://doi.org/10.12989/scs.2016.22.2.257

Jalaei, M. and Arani, A.G. (2018), "Size-dependent static and dynamic responses of embedded double-layered graphene sheets under longitudinal magnetic field with arbitrary boundary conditions", *Compos*. *Part B*: *Eng*., **142**, 117-130. https://doi.org/10.1016/j.compositesb.2017.12.053

Kar, V.R. and Panda, S.K. (2016), "Post-buckling behaviour of shear deformable functionally graded curved shell panel under edge compression", *Int*. *J*. *Mech*. *Sci*., **115**, 318-324. https://doi.org/10.1016/j.ijmecsci.2016.07.014

Kar, V.R. and Panda, S.K. (2017), "Postbuckling analysis of shear deformable FG shallow spherical shell panel under nonuniform thermal environment", *J*. *Thermal Stress*., **40**(1), 25-39. https://doi.org/10.1080/01495739.2016.1207118

Kar, V.R., Panda, S.K. and Mahapatra, T.R. (2016), "Thermal buckling behaviour of shear deformable functionally graded single/doubly curved shell panel with TD and TID properties", *Adv*. *Mater*. *Res*., *Int*. *J*., **5**(4), 205-221.

https://doi.org/10.12989/amr.2016.5.4.205
Kar, V.R., Mahapatra, T.R. and Panda, S.K. (2017), "Effect of different temperature load on thermal postbuckling behaviour of functionally graded shallow curved shell panels", *Compos. Struct.*, **160**, 1236-1247. https://doi.org/10.1016/j.compstruct.2016.10.125
Karami, B. and Janghorban, M. (2016), "Effect of magnetic field on the wave propagation in nanoplates based on strain gradient theory with one parameter and two-variable refined plate theory", *Modern Phys. Lett. B*, **30**(36), 1650421. https://doi.org/10.1142/S0217984916504212
Karami, B. and Janghorban, M. (2019), "Characteristics of elastic waves in radial direction of anisotropic solid sphere, a new closed-form solution", *Eur. J. Mech.-A/Solids*, **76**, 36-45. https://doi.org/10.1016/j.euromechsol.2019.03.008
Karami, B. and Karami, S. (2019), "Buckling analysis of nanoplate-type temperature-dependent heterogeneous materials", *Adv. Nano Res., Int. J.*, **7**(1), 51-61. http://dx.doi.org/10.12989/anr.2019.7.1.051
Karami, B. and Shahsavari, D. (2019), "Nonlocal strain gradient model for thermal stability of FG nanoplates integrated with piezoelectric layers", *Smart Struct. Syst., Int. J.*, **23**(3), 215-225. http://dx.doi.org/10.12989/sss.2019.23.3.215
Karami, B., Janghorban, M. and Li, L. (2018a), "On guided wave propagation in fully clamped porous functionally graded nanoplates", *Acta Astronautica*, **143**, 380-390. https://doi.org/10.1016/j.actaastro.2017.12.011
Karami, B., Janghorban, M. and Tounsi, A. (2018b), "Variational approach for wave dispersion in anisotropic doubly-curved nanoshells based on a new nonlocal strain gradient higher order shell theory", *Thin-Wall. Struct.*, **129**, 251-264. https://doi.org/10.1016/j.tws.2018.02.025
Karami, B., Shahsavari, D. and Janghorban, M. (2018c), "A comprehensive analytical study on functionally graded carbon nanotube-reinforced composite plates", *Aerosp. Sci. Technol.*, **82**, 499-512. https://doi.org/10.1016/j.ast.2018.10.001
Karami, B., Shahsavari, D., Nazemosadat, S.M.R., Li, L. and Ebrahimi, A. (2018d), "Thermal buckling of smart porous functionally graded nanobeam rested on Kerr foundation", *Steel Compos. Struct., Int. J.*, **29**(3), 349-362. http://dx.doi.org/10.12989/scs.2018.29.3.349
Karami, B., janghorban, M. and Tounsi, A. (2019a), "On exact wave propagation analysis of triclinic material using three-dimensional bi-Helmholtz gradient plate model", *Struct. Eng. Mech., Int. J.*, **69**(5), 487-497. http://dx.doi.org/10.12989/sem.2019.69.5.487
Karami, B., Janghorban, M. and Tounsi, A. (2019b), "Wave propagation of functionally graded anisotropic nanoplates resting on Winkler-Pasternak foundation", *Struct. Eng. Mech., Int. J.*, **70**(1), 55-66. http://dx.doi.org/10.12989/sem.2019.70.1.055
Karami, B., shahsavari, D., Janghorban, M. and Li, L. (2019c), "Influence of homogenization schemes on vibration of functionally graded curved microbeams", *Compos. Struct.*, **216**, 67-79. https://doi.org/10.1016/j.compstruct.2019.02.089
Karami, B., Shahsavari, D., Janghorban, M. and Li, L. (2019d), "Wave dispersion of nanobeams incorporating stretching effect", *Waves Random Complex Media*. https://doi.org/10.1080/17455030.2019.1607623
Karami, B., Shahsavari, D., Janghorban, M. and Tounsi, A. (2019e), "Resonance behavior of functionally graded polymer composite nanoplates reinforced with graphene nanoplatelets", *Int. J. Mech. Sci.*, **156**, 94-105. https://doi.org/10.1016/j.ijmecsci.2019.03.036
Karami, B., Shahsavari, D., Karami, M. and Li, L. (2019f), "Hygrothermal wave characteristic of nanobeam-type inhomogeneous materials with porosity under magnetic field", *Proceedings of the Institution of Mechanical Engineers, Part C: J. Mech. Eng. Sci.*, **233**(6), 2149-2169. https://doi.org/10.1177/0954406218781680
Katariya, P.V. and Panda, S.K. (2016), "Thermal buckling and vibration analysis of laminated composite curved shell panel", *Aircraft Eng. Aerosp. Technol., Int. J.*, **88**(1), 97-107. https://doi.org/10.1108/AEAT-11-2013-0202
Katariya, P.V., Panda, S.K., Hirwani, C.K., Mehar, K. and Thakare, O. (2017), "Enhancement of thermal buckling strength of laminated sandwich composite panel structure embedded with shape memory alloy fibre", *Smart Struct. Syst., Int. J.*, **20**(5), 595-605. http://dx.doi.org/10.12989/sss.2017.20.5.595
Katariya, P., Das, A. and Panda, S.K. (2018), "Buckling analysis of SMA bonded sandwich structure–using FEM", *Proceedings of IOP Conference Series: Materials Science and Engineering*, IOP Publishing, 012035.
Kiani, K. (2014), "Revisiting the free transverse vibration of embedded single-layer graphene sheets acted upon by an in-plane magnetic field", *J. Mech. Sci. Technol.*, **28**(9), 3511-3516. https://doi.org/10.1007/s12206-014-0811-1
Kim, S.-E., Thai, H.-T. and Lee, J. (2009), "A two variable refined plate theory for laminated composite plates", *Compos. Struct.*, **89**(2), 197-205. https://doi.org/10.1016/j.compstruct.2008.07.017
Kolahdouzan, F., Arani, A.G. and Abdollahian, M. (2018), "Buckling and free vibration analysis of FG-CNTRC-micro sandwich plate", *Steel Compos. Struct., Int. J.*, **26**(3), 273-287. http://dx.doi.org/10.12989/scs.2018.26.3.273
Lim, C.W. (2010), "On the truth of nanoscale for nanobeams based on nonlocal elastic stress field theory: equilibrium, governing equation and static deflection", *Appl. Math. Mech.*, **31**(1), 37-54. https://doi.org/10.1007/s10483-010-0105-7
Maluf, N. and Williams, K. (2004), *Introduction to Microelectromechanical Systems Engineering*, Artech House.
Mechab, I., Atmane, H.A., Tounsi, A. and Belhadj, H.A. (2010), "A two variable refined plate theory for the bending analysis of functionally graded plates", *Acta Mechanica Sinica*, **26**(6), 941-949. https://doi.org/10.1007/s10409-010-0372-1
Mehar, K., Mahapatra, T.R., Panda, S.K., Katariya, P.V. and Tompe, U.K. (2018), "Finite-element solution to nonlocal elasticity and scale effect on frequency behavior of shear deformable nanoplate structure", *J. Eng. Mech.*, **144**(9), 04018094. https://doi.org/10.1061/(ASCE)EM.1943-7889.0001519
Mehar, K., Panda, S.K., Devarajan, Y. and Choubey, G. (2019), "Numerical buckling analysis of graded CNT-reinforced composite sandwich shell structure under thermal loading", *Compos. Struct.*, **216**, 406-414. https://doi.org/10.1016/j.compstruct.2019.03.002
Murmu, T., McCarthy, M. and Adhikari, S. (2013), "In-plane magnetic field affected transverse vibration of embedded single-layer graphene sheets using equivalent nonlocal elasticity approach", *Compos. Struct.*, **96**, 57-63. https://doi.org/10.1016/j.compstruct.2012.09.005
Narendar, S. (2011), "Buckling analysis of micro-/nano-scale plates based on two-variable refined plate theory incorporating nonlocal scale effects", *Compos. Struct.*, **93**(12), 3093-3103. https://doi.org/10.1016/j.compstruct.2011.06.028
Narendar, S., Gupta, S. and Gopalakrishnan, S. (2012), "Wave propagation in single-walled carbon nanotube under longitudinal magnetic field using nonlocal Euler–Bernoulli beam theory", *Appl. Math.Model.*, **36**(9), 4529-4538. https://doi.org/10.1016/j.apm.2011.11.073
Nguyen-Van, H., Mai-Duy, N., Karunasena, W. and Tran-Cong, T. (2011), "Buckling and vibration analysis of laminated composite plate/shell structures via a smoothed quadrilateral flat shell element with in-plane rotations", *Comput. Struct.*, **89**(7),

612-625. https://doi.org/10.1016/j.compstruc.2011.01.005

Noor, A.K. (1975), "Stability of multilayered composite plates", *Fibre Sci. Technol.*, **8**(2), 81-89. https://doi.org/10.1016/0015-0568(75)90005-6

Pacoste, C. and Eriksson, A. (1997), "Beam elements in instability problems", *Comput. Methods Appl. Mech. Eng.*, **144**(1-2), 163-197. https://doi.org/10.1016/S0045-7825(96)01165-6

Panda, S. and Singh, B. (2013a), "Post-buckling analysis of laminated composite doubly curved panel embedded with SMA fibers subjected to thermal environment", *Mech. Adv. Mater. Struct.*, **20**(10), 842-853. https://doi.org/10.1080/15376494.2012.677097

Panda, S. and Singh, B. (2013b), "Thermal Postbuckling Behavior of Laminated Composite Spherical Shell Panel Using NFEM#", *Mech. Based Des. Struct. Mach.*, **41**(4), 468-488. https://doi.org/10.1080/15397734.2013.797330

Pasternak, P. (1954), "On a new method of analysis of an elastic foundation by means of two constants [Gosudarstvennoe Izdatelstvo Literaturi po Stroitelstvu I Arkhitekture]", Moscow: USSR.

Peddieson, J., Buchanan, G.R. and McNitt, R.P. (2003), "Application of nonlocal continuum models to nanotechnology", *Int. J. Eng. Sci.*, **41**(3-5), 305-312. https://doi.org/10.1016/S0020-7225(02)00210-0

Phan, N. and Reddy, J. (1985), "Analysis of laminated composite plates using a higher-order shear deformation theory", *Int. J. Numer. Methods Eng.*, **21**(12), 2201-2219. https://doi.org/10.1002/nme.1620211207

Pradhan, S. (2009), "Buckling of single layer graphene sheet based on nonlocal elasticity and higher order shear deformation theory", *Phys. Lett. A*, **373**(45), 4182-4188. https://doi.org/10.1016/j.physleta.2009.09.021

Pradhan, S. and Phadikar, J. (2009), "Nonlocal elasticity theory for vibration of nanoplates", *J. Sound Vib.*, **325**(1-2), 206-223. https://doi.org/10.1016/j.jsv.2009.03.007

Raghu, P., Preethi, K., Rajagopal, A. and Reddy, J.N. (2016), "Nonlocal third-order shear deformation theory for analysis of laminated plates considering surface stress effects", *Compos. Struct.*, **139**, 13-29. https://doi.org/10.1016/j.compstruct.2015.11.068

Rank, E., Krause, R. and Preusch, K. (1998), "On the accuracy of p-version elements for the Reissner-Mindlin plate problem", *Int. J. Numer. Methods Eng.*, **43**(1), 51-67. https://doi.org/10.1002/(SICI)1097-0207(19980915)43:1<51::AID-NME382>3.0.CO;2-T

Reddy, J.N. (2004), *Mechanics of Laminated Composite Plates and Shells: Theory and Analysis*, CRC press.

Reddy, J. and Phan, N. (1985), "Stability and vibration of isotropic, orthotropic and laminated plates according to a higher-order shear deformation theory", *J. Sound Vib.*, **98**(2), 157-170. https://doi.org/10.1016/0022-460X(85)90383-9

Sadoun, M., Houari, M.S.A., Bakora, A., Tounsi, A., Mahmoud, S. and Alwabli, A.S. (2018), "Vibration analysis of thick orthotropic plates using quasi 3D sinusoidal shear deformation theory", *Geomech. Eng., Int. J.*, **16**(2), 141-150. http://dx.doi.org/10.12989/gae.2018.16.2.141

Sayyad, A.S. and Ghugal, Y.M. (2015), "On the free vibration analysis of laminated composite and sandwich plates: A review of recent literature with some numerical results", *Compos. Struct.*, **129**, 177-201. https://doi.org/10.1016/j.compstruct.2015.04.007

Shahsavari, D. and Janghorban, M. (2017), "Bending and shearing responses for dynamic analysis of single-layer graphene sheets under moving load", *J. Brazil. Soc. Mech. Sci. Eng.*, **39**(10), 3849-3861. https://doi.org/10.1007/s40430-017-0863-0

Shahsavari, D., Karami, B., Janghorban, M. and Li, L. (2017), "Dynamic characteristics of viscoelastic nanoplates under moving load embedded within visco-Pasternak substrate and hygrothermal environment", *Mater. Res. Express*, **4**(8), 085013. https://doi.org/10.1088/2053-1591/aa7d89

Shahsavari, D., Karami, B., Fahham, H.R. and Li, L. (2018a), "On the shear buckling of porous nanoplates using a new size-dependent quasi-3D shear deformation theory", *Acta Mechanica*, **229**(11), 4549-4573. https://doi.org/10.1007/s00707-018-2247-7

Shahsavari, D., Karami, B. and Li, L. (2018b), "Damped vibration of a graphene sheet using a higher-order nonlocal strain-gradient Kirchhoff plate model", *Comptes Rendus Mécanique*, **346**(12), 1216-1232. https://doi.org/10.1016/j.crme.2018.08.011

Shahsavari, D., Karami, B. and Li, L. (2018c), "A high-order gradient model for wave propagation analysis of porous FG nanoplates", *Steel Compos. Struct., Int. J.*, **29**(1), 53-66. https://doi.org/10.12989/scs.2018.29.1.053

Shahsavari, D., Shahsavari, M., Li, L. and Karami, B. (2018d), "A novel quasi-3D hyperbolic theory for free vibration of FG plates with porosities resting on Winkler/Pasternak/Kerr foundation", *Aerosp. Sci. Technol.*, **72**, 134-149. https://doi.org/10.1016/j.ast.2017.11.004

She, G.-L., Ren, Y.-R., Yuan, F.-G. and Xiao, W.-S. (2018), "On vibrations of porous nanotubes", *Int. J. Eng. Sci.*, **125**, 23-35. https://doi.org/10.1016/j.ijengsci.2017.12.009

She, G.-L., Yuan, F.-G., Karami, B., Ren, Y.-R. and Xiao, W.-S. (2019), "On nonlinear bending behavior of FG porous curved nanotubes", *Int. J. Eng. Sci.*, **135**, 58-74. https://doi.org/10.1016/j.ijengsci.2018.11.005

Shimpi, R.P. (2002), "Refined plate theory and its variants", *AIAA Journal*, **40**(1), 137-146. https://doi.org/10.2514/2.1622

Shimpi, R. and Patel, H. (2006), "A two variable refined plate theory for orthotropic plate analysis", *Int. J. Solids Struct.*, **43**(22-23), 6783-6799. https://doi.org/10.1016/j.ijsolstr.2006.02.007

Singh, S., Singh, J. and Shukla, K. (2013), "Buckling of laminated composite plates subjected to mechanical and thermal loads using meshless collocations", *J. Mech. Sci. Technol.*, **27**(2), 327-336. https://doi.org/10.1007/s12206-012-1249-y

Stamoulis, K. and Giannakopoulos, A. (2012), "A study of size effects and length scales in fracture and fatigue of metals by second gradient modelling", *Fatigue Fract. Eng. Mater. Struct.*, **35**(9), 852-860. https://doi.org/10.1111/j.1460-2695.2012.01668.x

Thai, H.-T. and Kim, S.-E. (2010), "Free vibration of laminated composite plates using two variable refined plate theory", *Int. J. Mech. Sci.*, **52**(4), 626-633. https://doi.org/10.1016/j.ijmecsci.2010.01.002

Thai, H.-T. and Kim, S.-E. (2012), "Analytical solution of a two variable refined plate theory for bending analysis of orthotropic Levy-type plates", *Int. J. Mech. Sci.*, **54**(1), 269-276. https://doi.org/10.1016/j.ijmecsci.2011.11.007

Wang, X., Shen, J., Liu, Y., Shen, G. and Lu, G. (2012), "Rigorous van der Waals effect on vibration characteristics of multi-walled carbon nanotubes under a transverse magnetic field", *Appl. Math. Model.*, **36**(2), 648-656. https://doi.org/10.1016/j.apm.2011.07.017

Winkler, E. (1867), "Die Lehre von Elastizitat und Festigkeit (The theory of elasticity and stiffness)", H. Domenicus, Prague, Czech Republic.

Zhang, Y., Liu, G. and Xie, X. (2005), "Free transverse vibrations of double-walled carbon nanotubes using a theory of nonlocal elasticity", *Phys. Rev. B*, **71**(19), 195404. https://doi.org/10.1103/PhysRevB.71.195404

Zidi, M., Tounsi, A., Houari, M.S.A. and Bég, O.A. (2014), "Bending analysis of FGM plates under hygro-thermo-mechanical loading using a four variable refined plate theory",

Aerosp. Sci. Technol., **34**, 24-34.
https://doi.org/10.1016/j.ast.2014.02.001

CC